Management zone delineation using a modified watershed algorithm [★]

Pierre Roudier [a,b,*], Bruno Tisseyre [c], Hervé Poilvé [b],
Jean-Michel Roger [a]

[a]*Cemagref, 361 rue J.F. Breton, BP 5095, F-34196 Montpellier Cedex 05*
[b]*Infoterra France, 31 rue des Cosmonautes, F-31402 Toulouse Cedex 04*
[c]*Montpellier SupAgro, 2 place Viala, 34060 Montpellier Cedex 01, France*

Abstract

Site-specific management (SSM) is a common way to manage within-field variability. This concept divides fields into site-specific management zones (SSMZ) according to one or several soil or crop characteristics. This paper proposes an original methodology for SSMZ delineation which is able to manage different kinds of crop and/or soil images using a powerful segmentation tool: the watershed algorithm. This image analysis algorithm was adapted to the specific constraints of precision agriculture. The algorithm was tested on high-resolution bio-physical images of a set of fields in France.

Key words: Management zones, Remote sensing, Image analysis, Watershed segmentation

Introduction

Within-field variability is a well-known phenomenon in agriculture, and its study is at the centre of precision agriculture (PA). The most common method to manage this phenomenon is the site-specific management (SSM) concept (Plant, 2001). The principle of this concept is to manage areas within a field with variable rates of input (Godwin et al., 2003). Site-specific management zones (SSMZ) can be defined in

hal-00453898, version 1 - 5 Feb 2010

a given field in order to manage within-field variability. A management zone is a sub-region of a field which is defined by a relative homogeneity of crops and/or soil parameters (Doerge, 1999), and for which a specific rate of inputs is needed. This within-field heterogeneity management method represents a major development for decision support systems (DSS, McBratney et al., 2005).

Farmstar (Coquil and Bordes, 2005) is a DSS based on remote-sensing data which is proposed in France by Infoterra and Arvalis. This service, which has been operational for six years in most of the significant cereal-growing regions, provides farmers with a series of recommendations to monitor crops at the within-field level. Farmstar combines satellite imagery, agronomic models and meteorological data, and was used in France by more than 9,000 farmers for 350,000 ha in 2007. This study aims at finding suitable SSMZ delineation strategies for a widespread DSS like Farmstar.

In the PA literature, various methodologies for SSMZ delineation can be found. A majority of the existing methods are based on unsupervised clustering algorithms (Vrindts et al., 2005). Fraisse et al. (1999) used an ISODATA clustering algorithm. Several authors proposed to use the k-means algorithm (Taylor et al., 2003; Whelan and McBratney, 2003; Hornung et al., 2006). Finally, the fuzzy c-means algorithm is now widely applied (Lark and Stafford, 1997; Fridgen et al., 2000; Vrindts et al., 2005; Li et al., 2007). The expansion of the latter approach has been made easier for researchers with the release of user-friendly software like Management Zone Analyst (Fridgen et al., 2004). The choice of the data layers that are processed by the clustering algorithm has been widely discussed (for more detail, the reader can refer to Jaynes et al., 2005; Miao et al., 2005). Despite their success, some authors noticed that a major drawback of the existing approaches is the resulting fragmentation of the zones. This fragmentation is due to the fact that no spatial information is taken into account in the clustering algorithms (Ping and Dobermann, 2003; Simbahan and Dobermann, 2006; Frogbrook and Oliver, 2007). This effect may be reduced by applying a spatial filter on the result of a fuzzy c-means clustering (Ping and Dobermann, 2003; Lark, 1998). Li et al. (2005) presented a modified version of the k-means clustering algorithm so that it considers both spatial relationships and similarities among pixels. Khosla et al. (2002) proposed to include user-defined polygons alongside crop and soil information layers. Simbahan and Dobermann (2006) and Frogbrook and Oliver (2007) proposed to introduce a spatial constraint through the variogram parameters. This overview of the literature on SSMZ delineation tools shows that existing approaches (i) rarely consider DSS mass-production constraints, and (ii) are mostly classification-based.

Implementing SSMZ support in a production context implies finding new techniques for SSMZ definition. A mass-production context defines new constraints and legitimizes a specific research effort. Robustness is an important point (McBratney et al., 2005), because (i) the delineation method has to be suitable for a wide range of agro-meteorological conditions, and (ii) the method should also be suitable for

2

different kinds of data layer. Due to the large amount of data to be processed, specific constraints appear, mostly automation and computing efficiency. One should also consider that only remotely-sensed data is processed, *i.e.* data on a regular grid. In this study, an original approach for SSMZ delineation, using a segmentation tool instead of classification methods, is proposed. An innovative method has been built to address the drawbacks of classification-based methods: spatial fragmentation, control of the resulting number of patches, operations on the morphological characteristics of the patches. Specific constraints presented above like automation, robustness and computing-time are considered. An adaptation of an efficient image-processing segmentation tool to the requirements presented above is proposed. In-field experiments have been carried out on a set of fields in the Burgundy region, France, and show promising results for segmentation-based SSMZ delineation methods.

Theory

Presentation of the watershed segmentation algorithm

SSMZ delineation methods are mostly based on classification tools (Vrindts et al., 2005). In this paper, a segmentation method for SSMZ definition is proposed. Classification gathers the similar pixels of an image according to their radiometrical value, whereas segmentation aims at defining homogeneous zones, and is based on how the values are spatially structured (*i.e.* topology of the dataset): classification defines classes, *i.e.* groups of individuals presenting similar properties, and segmentation defines regions, *i.e.* the expression of those groups in space and/or time (McBratney et al., 2005). The proposed method is based on the detection of the boundaries of the SSMZ in the processed images.

Mathematical morphology (Serra, 1982) proposes an efficient segmentation method, *i.e.* the watershed algorithm. This is a low-level segmentation method initially proposed by Beucher and Lantuejoul (1979) and formalized later by Vincent and Soille (1991). This algorithm is fast and generates closed contours. It has been used on various kinds of images. It is based on an analysis of the magnitude of the gradient image: effective contours correspond to high gradient values. The gradient image can be seen as a hilly landscape, the edges of the hills being the contours of the objects to segment. An iterative flooding of this landscape from the local minima is simulated (Figure 1). The contours of the objects to segment are defined as the points where different flooding lakes meet. A dam between those different lakes is built to mark the contours of the objects.

As the method is based on the gradient magnitude image, it is very sensitive to noise, and over-segmentation of the image is a major drawback of the watershed
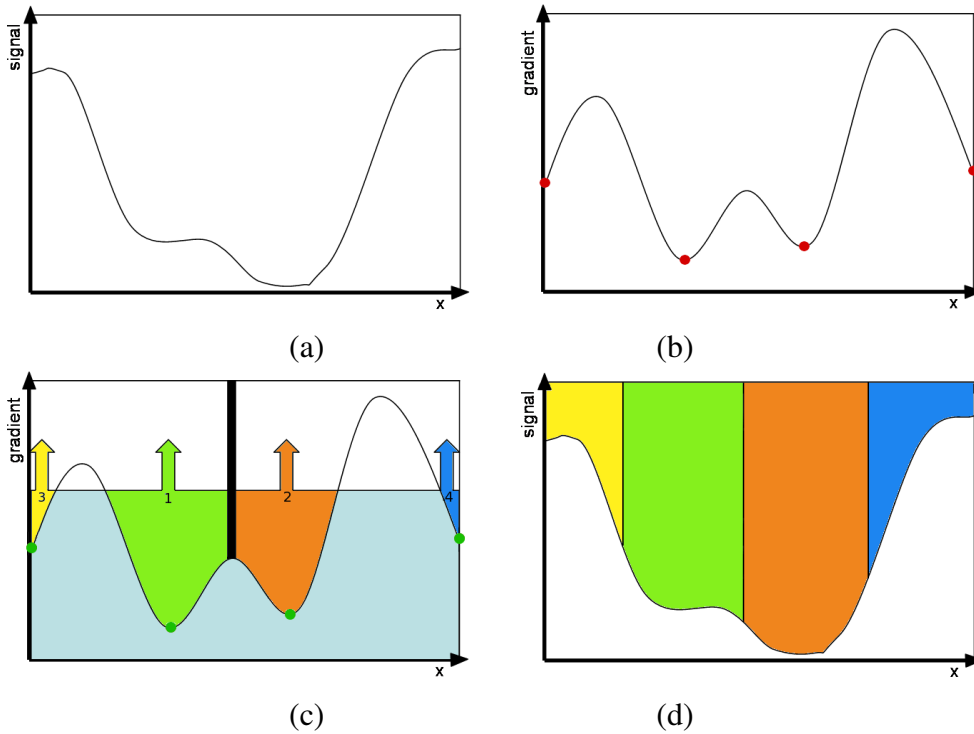
3

Fig. 1. One dimensional illustration of the watershed segmentation. (a) The signal to be segmented. (b) The corresponding gradient signal. Local minima are plotted in red. (c) Flooding of the grey levels from each local minima. When two different floods meet, a dam is built up. Those dams are the resulting contours of the segmentation. (d) Resulting segmentation of the signal.

segmentation (Najman and Schmitt, 1996). The over-segmentation phenomenon relates to the creation of small non-representative basins. To solve this problem, a region-merging algorithm is commonly applied after watershed segmentation (Haris et al., 1998; Patino, 2005; Pichel et al., 2006). Another way to limit the over-segmentation phenomenon is to initiate relevant basin seeds (Meyer and Beucher, 1990). Finally, some authors have proposed characterizing the strength of the different detected contours (Grimaud, 1992; Najman and Schmitt, 1996).

Grimaud (1992) proposed selecting the relevant basin seeds using the basin dynamic method: for a given local minima k of a basin B, the basin dynamic D is defined as the difference between the altitude of k and the lowest altitude to be overcome to gain access to a lower local minimum k (Figure 2). The basin dynamics hierarchize watershed seed candidates, and the basin dynamics map is thresholded so that relevant seeds are selected. However, choosing a threshold is an empirical exercise. The method presented in this paper was inspired from this approach. Here the basin dynamics method is modified by introducing a variable in the standard watershed algorithm itself, in order to improve its robustness to over-segmentation and adapt to the scientific framework of PA. In the PA context, data are often affected by different noise sources (noise due to the sensor and/or the process applied to the data, nugget effect, etc.). It is important to provide a strategy to reduce the
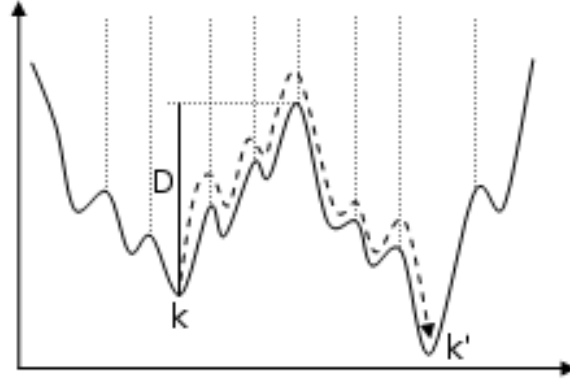
4

Fig. 2. One dimensional illustration of the concept of basin dynamics. In this example, D is the dynamic of the basin seed *k*.

incidence of such effects, because they generate an important number of small non-significant zones using an algorithm like the watershed algorithm. The originality of our work is to provide a non-parametric method to compute the over-segmentation regulation variable in order to fit with our production context.

Proposition of a specific watershed algorithm for SSMZ delineation

There are two important steps in watershed segmentation. The first step is "diffusion", and consists in the propagation of the existing regions pixel by pixel. The second step is called "labellization", it involves the creation of a new region. Thus, over-segmentation is actually the result of over-labellization. In the standard formulation of the algorithm, those two steps are simultaneous. A "flooding lag" Δ_f is introduced in the standard watershed algorithm between diffusion and labellization, so that labellization and diffusion steps are staggered. The objective of this lag is to maximize the diffusion step, *i.e.* the spreading of the existing regions, to the detriment of the creation of non-significant zones (Figure 3).

The algorithm processes a gradient image G and generates an image of watershed labels WS, initialized at 0. Two lists of pixels are updated at each step *k* of the segmentation loop:

$$ik = \{i \in G \,|\, G(i) \leq k,\, WS(i) = 0\} \tag{1}$$

$$iks = \{i \in G \,\big|\, G(i) = (k - \Delta_f),\, WS(i) = 0\} \tag{2}$$

The *ik* list is defined as the pixels that can be allocated to the existing basins. This list groups all the unlabeled pixels whose gradient is smaller or equal to *k*. The second list, *iks*, is more restrictive. It gathers all the unlabeled pixels whose gradient equals $k - \Delta_f$. Thus, by definition, *iks* is included in *ik*. In a given step of the segmentation process, diffusion inside the list *ik* is computed first. An iterative loop allows the unlabeled pixels to be allocated to the same label as their neighbour, as
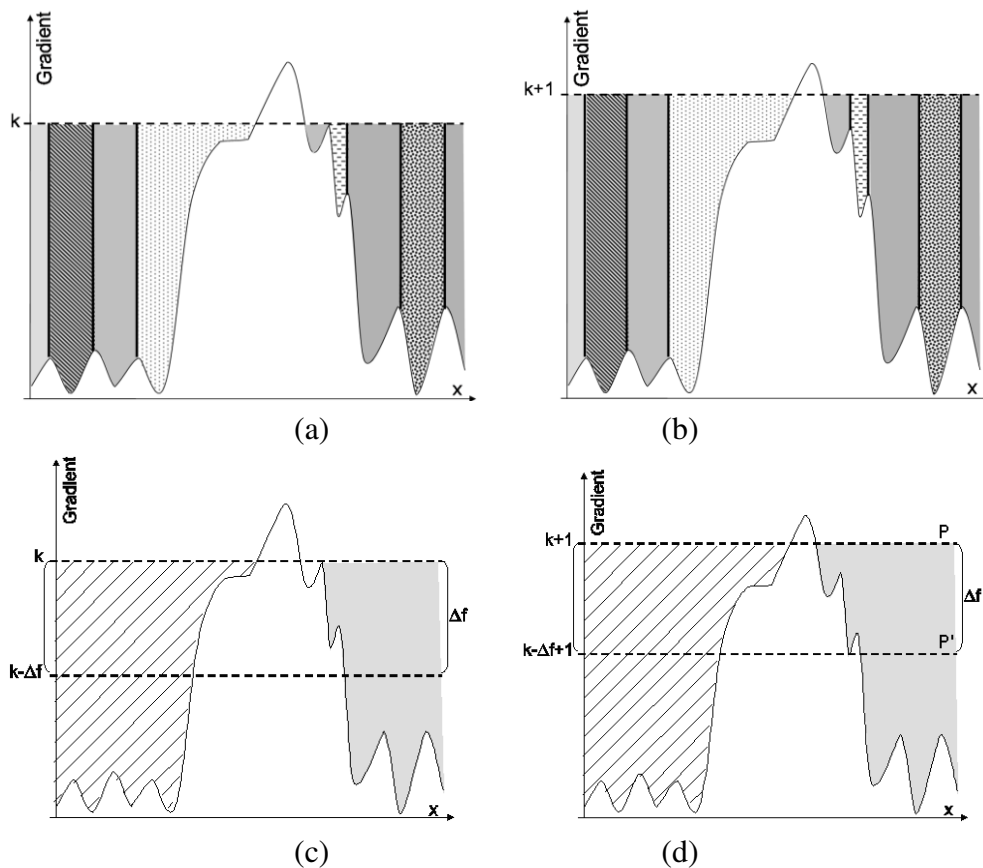
5

Fig. 3. One dimensional illustration of our approach. Plain line represents the gradient magnitude, which is used to detect contours, for one spatial dimension (x). (a, c) Iteration k for the standard watershed algorithm and our approach respectively. (b, d) Iteration $k+1$ for the standard watershed algorithm and our approach respectively. Diffusion of the existing regions takes place in the volume between $(k+1)$ and $(k-\Delta_f+1)$, *i.e.* between P and P' (Δ_f is the flooding lag). Creation of new regions only occurs on the $(k-\Delta_f+1)$ plane, *i.e.* P'. Over-segmentation due to noisy basins is limited while significant gradient values are respected.

long as the latter has been labelled itself. If several labels are candidates, the neighbour having the closest value in the initial image is chosen. The processed pixels are eliminated from the *ik* list. At the end of the diffusion step, the *ik* list may or may not be empty. When all the possibilities of diffusion inside *ik* have been processed, the *iks* list is generated. All the pixels which have not yet been allocated to a basin and whose gradient equals $k-\Delta_f$ are compiled within this list. As it was not possible to give them a label during Δ_f steps, it was decided to move on to the next step *i.e.* creation of new basins, considered to be significant. The first item on the list is given a new label, thereby creating a new basin. This label is then diffused among the pixels contained in the *ik* list. The labelled pixels are then removed from *iks* list. The creation of new basins is repeated until *iks* is empty.

During the two steps of the process (Figure 3), the algorithm compiles two separate lists of pixels. List *ik* is the diffusion volume V defined between the plane P of the

6

current gradient value k, and the plane P, shifted of Δ_f from P. The *iks* list is defined by the unlabeled pixels of plane P. The *iks* list is the only plane used for the creation of new basins (labellization step). The treatment of pixels that were not labelled by simple diffusion is thereby forced.

Assessment of the flooding lag Δ_f

The specificity of our watershed algorithm relies on the introduction of a flooding lag Δ_f between diffusion and labellization. This limits the over-segmentation effect by limiting the creation of new regions. Δ_f can be determined by an empirical or expert method. However, in order to reduce operator interventions and expertise, a method that gives Δ_f from the intrinsic characteristics of the data to be segmented is proposed.

On the gradient image to be processed, one should distinguish low spatial frequency variations, which are due to the border between two significant objects, from high spatial frequency variations, which can be due to noise. The detection and the estimation of this noise can be carried out by studying the local variations of the variance in the gradient image. Thus, let σ_N be a measurement of the high spatial frequency noise on the gradient image. Δ_f is proportional to σ_N:

$$\Delta_f = k \times \sigma_N, \ k \in \mathbb{R} \tag{3}$$

σ_N can be estimated using the square root of the average variance of the high spatial frequency noise on the gradient image. Let V_0 be this variance. As the disturbances that give rise to over-segmentation are local phenomena, V_0 can be defined, for a gradient image G, as the limit of the average variance $\overline{V}$ on surfaces S when S tends toward 0:

$$V_0 = \lim_{S \to 0} \overline{V}(G(S)) \tag{4}$$

$$\widehat{\sigma_N} = \sqrt{V_0} \tag{5}$$

$$\Delta_f = k' \times \sqrt{V_0}, \ k' \in \mathbb{R} \tag{6}$$

Due to the way it is computed (Equation 5), the standard deviation σ_N is an average of the image. However, from one case to another, the gradient image for which it has been computed can present a distribution of high spatial frequency phenomena which are more or less homogeneous. If those phenomena are not uniformly distributed over the image —and are thus spatially structured— it means that the areas with high spatial frequency phenomena may be meaningful (*e.g.* textured areas). To avoid under-segmentation of such heterogeneous meaningful structures, it is important to take into account the levelling effect of the mean operator. Consequently, in

7

the case of heterogeneous noise structuring images, the flooding lag Δ_f must be reduced to avoid under-segmentation of those areas of the image to be segmented.

Let V_T be the total variance of the gradient image. V_T can be seen as the mean variance, on the whole gradient image, for two distant points. In the case of a homogeneous gradient image, $V_T \approx V_0$, the mean variance between two distant points is similar to the mean variance of two neighbouring points, as noise distribution is homogeneous. In the case of a heterogeneous gradient image, $V_0 << V_T$, two neighbouring points will on average be closer in value than two distant points, because the noise distribution is spatially structured. The ratio between V_0 and V_T can be used to evaluate the heterogeneity of noise distribution in the gradient image:

- If the gradient image presents a homogeneous distribution of these phenomenon, then $V_0 \approx V_T$ and $V_0/V_T \to 1$. This kind of distribution does not require a decrease in the flooding lag.
- If the gradient image shows a heterogeneous distribution of these phenomenon, then $V_0 << V_T$ and $V_0/V_T \to 0$. Such a distribution requires a significant decrease in the flooding lag to avoid under-segmentation.

A weighting factor k, proportional with a real constant K to the ratio V_0/V_T can be proposed. The flooding lag Δ_f is estimated (Equation 3) by:

$$
\begin{aligned}
\Delta_f &= k' \times \sqrt{V_0} \\
&= \left(K \times \frac{V_0}{V_T} \right) \times \sqrt{V_0}, \; K \in \mathbb{R}
\end{aligned}
\tag{7}
$$

Thereafter, a constant $K = 1$ is used.

Material and methods

Study sites and data collection and processing

The study sites were four arable crop-fields located on commercial farms in Burgundy, an important cereal-growing region, near Dijon, France. The soil of those four fields is a silty loam. In terms of area, the sampled sites included two average fields, between 15 and 20 ha (Table 1, fields 1 and 2), and two larger fields (Table 1, fields 3 and 4). The four fields were cropping three different winter wheat (Triticum æstivum) varieties (Table 1). The data collection on those fields took place in 2003. For each field, the opportunity index (OI, Pringle et al., 2003) was computed to qualify the within-field variability. The opportunity index is defined as a function of the magnitude of the data variation (assessed by CV_a), and of the spatial structure of the data variation (assessed by S).

Fields characteristics			Biomass at flowering (t/ha)				Spatial statistics		
Field	Size (ha)	Variety	Min.	Max.	Mean	St. Dev.	CV_a	S	OI
1	15.3	Apache	3.67	11.25	8.45	1.54	0.18	0.86	0.16
2	17.5	Charger	4	16.21	10.25	3.39	0.34	0.79	0.27
3	30.3	Apache	1.65	13.15	9.67	1.38	0.15	0.68	0.10
4	69.5	Soissons	3.62	11.86	7.27	1.54	0.25	0.69	0.17

Table 1

Details of the four study sites.

The remotely-sensed data used for the experiments were acquired using an airborne CASI sensor mounted on a jet. 11 spectral bands were used, centred at 444, 487, 555, 623, 668, 693, 716, 738, 783, 852, and 900 nm respectively, with a spatial resolution of 5m. Acquisitions were done by the Institut Cartogràphic de Catalunya (ICC), on May 30, 2003, so that the wheat was during the flowering growth stage. The multi-spectral data were processed in order to obtain biomass data on the four experimental fields. The process to provide biomass maps was done using the Farm-star production chain (Poilvé and Coquil, 2003). Table 1 describes field area, wheat variety and statistics of the estimated biomass values.

Biomass data pre-processing

The gradient operator is the morphological gradient, with a square structural element 3×3 (Rivest et al., 1993). For an image I, it is computed as follows:

$$g(I) = \delta_E(I) - \varepsilon_E(I) \tag{8}$$

where δ is the dilatation morphological operator and ε the dilatation morphological operator (Serra, 1982).

Utilisation of the variogram for the determination of Δ_f

The estimation of V_0 can be done by studying the local variations of the variance in the gradient image. Thus, one can estimate V_0 using different methods: variographic analysis, Fourier analysis, wavelets, etc. In this study, the variogram method (Matheron, 1963; Journel and Huijbregts, 1978) was chosen to estimate the value of V_0 by the nugget effect C_0 of the variogram (Equation 9). This method estimates V_0 and V_T by considering the relation between the variance of a set of points and the physical distance between them. Modelling of the experimental variogram allows the estimation of the variance for a null distance between two points. The variogram

9

model provided two variables C_0 and C_1. The total variance of the image V_T was obtained through addition of C_0 and C_1 (Equation 10). Considering relation 7, Δ_f is computed as presented in relation 11.

$$\widehat{V_0} = C_0 \tag{9}$$
$$\widehat{V_T} = C_0 + C_1 \tag{10}$$
$$\Delta_f \approx \frac{C_0}{C_0 + C_1} \times \sqrt{C_0} \tag{11}$$

Regularisation of the number of zones

In order to refine the results of the watershed segmentation, a regularisation of the watershed segmentation result is done. In image processing, regularisation is the step that aims at improving the results of a segmentation. Indeed, our watershed implementation keeps a small over-segmentation effect, and needs a region merging step to reach the suitable number of regions. This corresponds to the under-segmentation risk management of our approach, which is formulated by the term $\left(\frac{C_0}{C_0 + C_1}\right)$ in the Δ_f expression (Equation 11).

In this study, a hierarchical tree algorithm was used to drive the regularisation process. Figure 4 shows a one-dimensional illustration of this fusion procedure. The initial state (IS) corresponds to the regions resulting from the segmentation step. The fusion is only performed between neighbouring regions. All the fusions that are possible between the neighbouring regions are evaluated. The most favorable fusion is operated using a fit parameter, which is an energy function. This operation is repeated until the suitable number of regions is obtained.

The fit parameter considers both morphological and radiometric parameters. For a given fusion, the fit parameter is a linear combination of compactness (C), regularity (R) and radiometry ρ (Table 2, for more information see Baatz and Schäpe, 2000). For a given region, when several fusions with neighbouring regions are possible, the one which minimizes the fit parameter is processed.

Determination of the optimum number of zones

The choice of the best number of zones is done for each field. It is based on a variance analysis of the biomass values inspired from Fraisse et al. (1999). Biomass variances for each zone were computed (Equation 12):

$$V_{INTRA} = \sum_{Z=1}^{N} \sum_{i=1}^{n_Z} \left(B_i - \overline{B_Z} \right)^2 \tag{12}$$
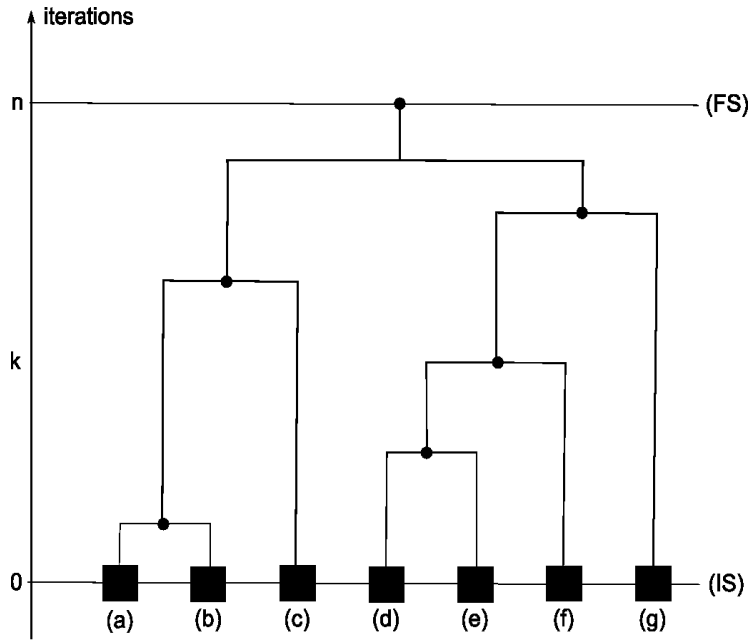
10

Fig. 4. Tree algorithm used to merge regions according to a given fit parameter. In this one dimensional example, at the initial state (IS), there were eight different regions. The tree algorithm examines all the possible fusions between the different couples of neighbours. At each iteration, the best fusion according to the fit parameter is chosen. The process is repeated until a given number of regions k, or until one region (final state, FS), is obtained.

Parameter	Assessed characteristic	Formula
Compactedness (C)	Morphological	$C = \dfrac{P_{region}}{\sqrt{S_{region}}}$
Regularity (R)	Morphological	$R = \dfrac{P_{region}}{P_{BBox}}$
Radiometry (ρ)	Radiometric	$\rho = \sqrt{\dfrac{\Sigma[Biomass(k)]^2 - \frac{[\Sigma Biomass(k)]^2}{S_{region}}}{S_{region}}}$

$$Fit = (k_1 \times C) + (k_2 \times R) + (k_3 \times \rho), \ k_{\{1,2,3\}} \in \mathbb{R}, \ \Sigma_{i=1}^{3} k_i = 1$$

Table 2

Composition of the fit parameter within the hierarchical tree algorithm. P_{region} is the perimeter of the region, S_{region} is its surface. P_{BBox} is the perimeter of the bounding box of the region.

N is the number of zones, n_Z the number of cells in the zone Z, B_i the biomass value for cell i, and $\overline{B_Z}$ the mean of biomass for zone Z. The percentage decrease in within-zone biomass variance (with reference to the entire field, *i.e.* one unique zone) was plotted versus the number of zones (Figure 5). To find the most suitable number of zones, the parsimony principle, described by Lark (2001) for PA, was applied to each plot. According to this principle, the most suitable number of zones is defined as the number of zones after which the biomass variance reduction remains more or less constant or declines more slowly.
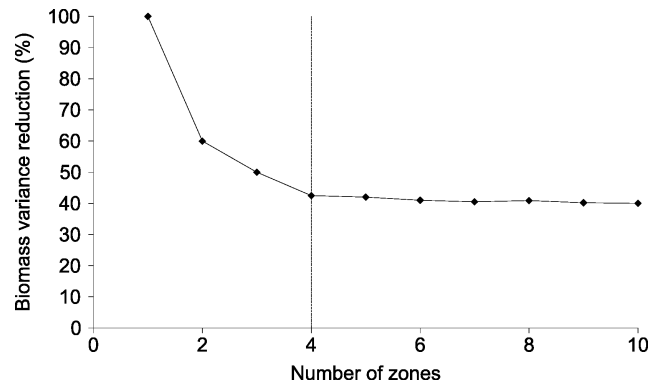
11

Fig. 5. Illustration of the application of the parsimony principle to the choice of the final number of regions. Biomass variance decrease (%) is plotted versus the number of regions when dividing the field into 1 to 10 SSMZ. The parsimony principle leads to a choice of $N = 4$.

Data analysis

The algorithms proposed in this paper were implemented using the IDL programming language (IDL 6.2, 2005, © Research Systems, Inc., USA), on a PC platform running on an Intel Pentium 4 processor at 2.8 Ghz and with 1 Gb RAM. Both exponential and spherical variogram models were used (Webster and Oliver, 1990). Variographic computations were processed with the Vesper software (Minasny et al., 2005). The performance of the variographic modelling was determined with the RMSE. A flow chart (Figure 6) summarizes the different steps of our method.

Results

Assessment of the flooding lag

Experimental variograms were computed for each field from the gradient of the biomass maps. Figure 7 shows the processed gradient data, the corresponding experimental variograms (dots) and the fitted variogram model (plain line). The parameters of the models fitted are also shown in Table 3. For each field, stationarity was obtained for the fitted model.

In the Δ_f assessment method using a variogram model of the gradient data, important parameters are the nugget effect C_0 and sill C_1. Within our experimental fields set, Field 3 is the field with the lowest Δ_f: the nugget effect is low, because there are few high spatial frequency noise effects. Moreover, the ratio between C_0 and $C_0 + C_1$ is low, and thus the Δ_f value is lowered in order to avoid under-segmentation phenomena. Indeed, this field (Figure 7) shows numerous zones, and
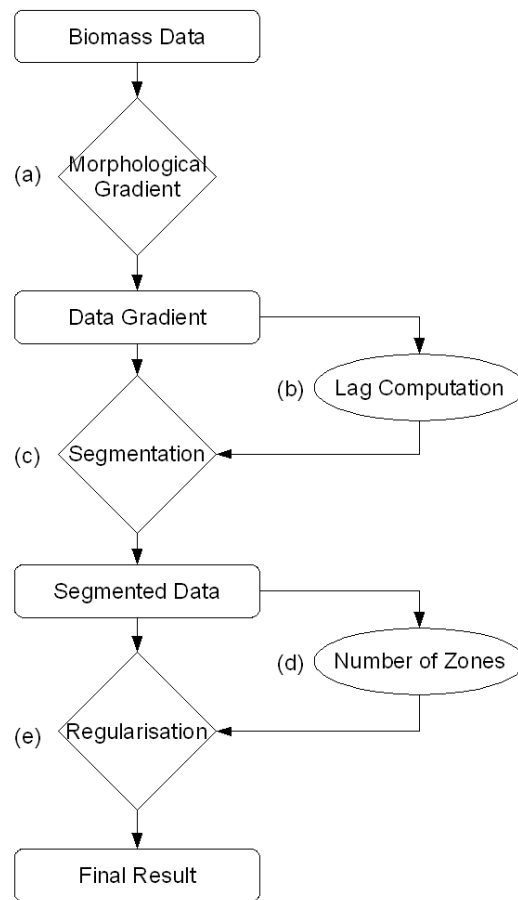
12

Fig. 6. Flow chart of the proposed approach. (a) The morphological gradient of the biomass map to be processed is computed. (b) Flooding lag Δ_f is computed from the morphological gradient of the biomass map. (c) The biomass map is segmented from its gradient, using the modified watershed algorithm presented above with the flooding lag Δ_f computed in the (b) step. (d) The most suitable final number of zones is chosen. (e) The number of zones is reduced using the regularisation algorithm.

magnitude between zones is not important (Table 1, $CV_a = 0.15$). Conversely, Field 2 shows a high Δ_f value: an important nugget effect allowed us to take no account of most of the local variations in the gradient map, and the Δ_f value was not lowered by the $C_0/(C_0 + C_1)$ ratio. Figure 7 shows that this field presents a small number of wide and well-marked SSMZ.

Field	Model	h_{max} (m)	C_0	C_1	RMSE	Δ_f (t/ha)
1	Spherical	550	1364.5	1243.9	121.0	0.56
2	Exponential	650	1769.9	1665.5	121.3	1.02
3	Exponential	800	577.2	1878.2	65.71	0.25
4	Exponential	1000	861.3	705.4	24.64	0.47

Table 3

Results of the Δ_f assessment using a variogram analysis for the 4 experimental fields.
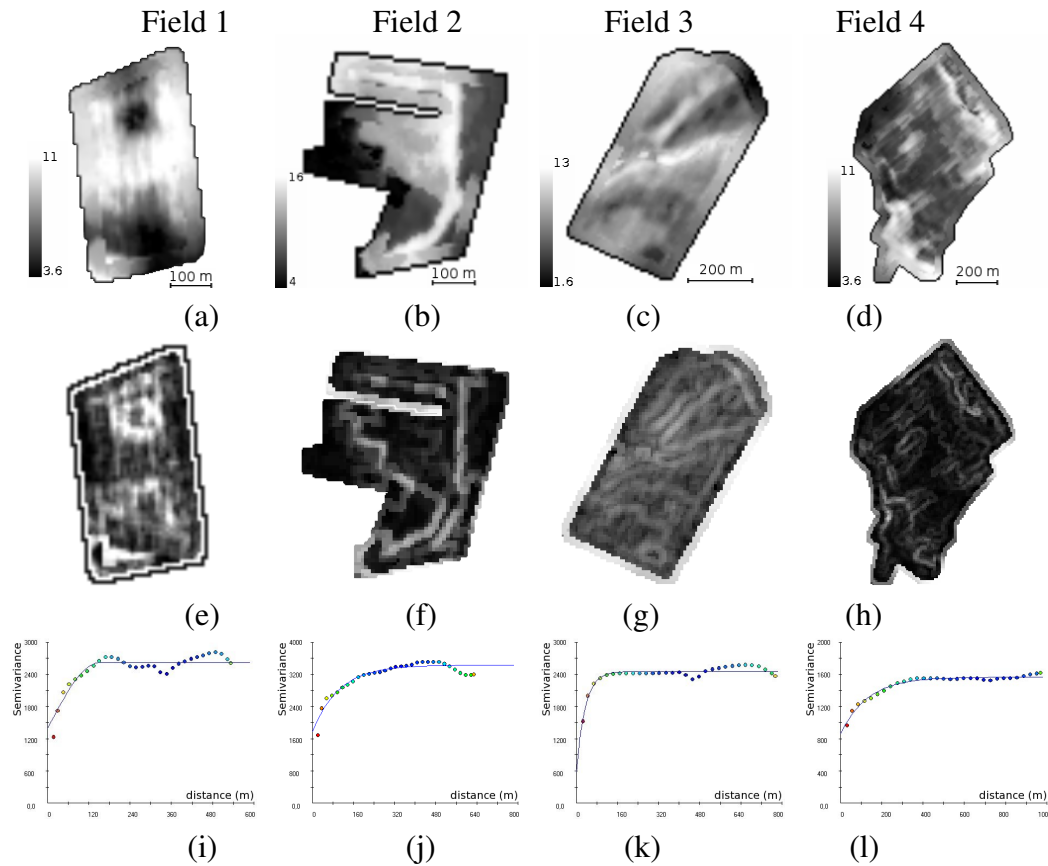

Fig. 7. Variograms on the gradient data for the four experimental fields. (a – d) Biomass maps (t/ha) for fields $\{1, 2, 3, 4\}$ respectively. (e – h) Gradient of the biomass maps for fields $\{1, 2, 3, 4\}$ respectively. (i – l) Variograms of the gradient map for fields $\{1, 2, 3, 4\}$ respectively.

Reduction of the over-segmentation using our watershed algorithm

Figure 8 shows the contours of the SSMZ delineated on Field 4 before the regularisation step, using the standard watershed algorithm on the one hand, and our watershed algorithm improved with flooding lag Δ_f on the other hand. An important reduction of the number of zones is observed when using the flooding lag watershed segmentation method. The latter method delineated wider, more significant

14

zones, while the standard algorithm is strongly affected by the over-segmentation phenomenon. Table 4 compares some quantitative statistics: for the two methods, the number of delineated zones and the average area of those zones is shown.
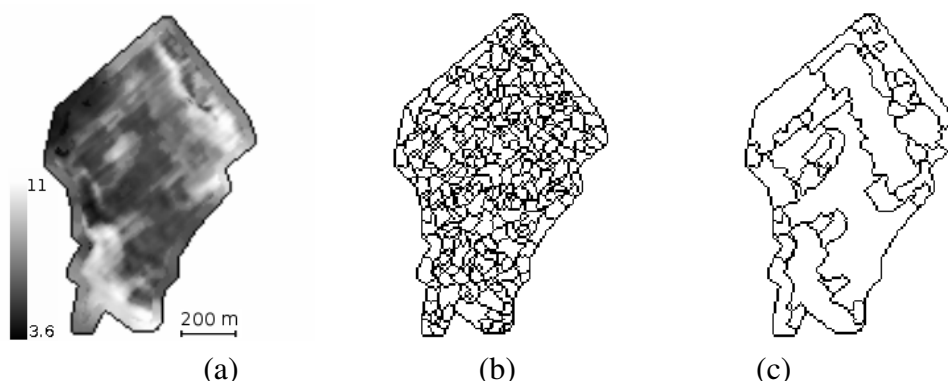

| | (a) | (b) | (c) |

Fig. 8. Comparison of the watershed segmentation results on the experimental field 4. (a) Biomass values (t/ha). (b) Segmentation results using the standard watershed algorithm. (c) Segmentation results using our approach.

Field	Number of zones		Average area (ha)	
	without Δ_f	with Δ_f	without Δ_f	with Δ_f
1	95	8	0.20	2.44
2	105	25	0.24	1.00
3	161	45	0.23	0.81
4	349	41	0.23	1.94

Table 4

Comparative results of the watershed segmentation step using the standard watershed algorithm and our watershed algorithm with a flooding lag Δ_f: number of delineated zones and average area of the delineated zones.

Results show that there is an important reduction of the number of delineated zones: between 72 and 91.6% for the tested fields. Consequently, the average area of the delineated objects is much more important when using our watershed algorithm. Those two results correspond to the objective of reduction of the over-segmentation phenomenon, in order to work on objects containing a significant number of pixels. As a result, zones given by our algorithm are more relevant, and split the field into homogeneous regions. However, an over-segmentation effect is still observed, and corresponds to the under-segmentation risk-management policy of our method.

Figure 9 compares the result of the SSMZ delineation on Field 4, using the standard watershed algorithm on the one hand and the proposed flooding lag watershed algorithm on the other hand. The same regularisation step was applied to both segmentation results presented in Figure 8. The SSMZ delineations obtained present the same number of regions, but the contours of the regions are different depending on the watershed segmentation algorithm used. When using the standard watershed

15

algorithm, contours are tortuous and complex, and follow the finest spatial variations of the biomass. When using the over-segmentation limitation method, the result gives a more global and simple view of the within-field variations. Indeed, the contours are less complex and render the most significant spatial variations of the biomass. As a result, the latter suits expectations of the project, which is to provide farmers a simplified visualisation of their field variability. This difference underlines the necessity to restrict over-segmentation in the first step. In the case of the standard watershed algorithm, the important initial over-segmentation (Figure 8) implies that the regularisation algorithm processes very small patches, at a scale closer to the data resolution scale (Table 4). Conversely, the over-segmentation limitation method using a flooding lag allows the regularisation step to process wider objects: this segmentation algorithm is more efficient in terms of taking into account spatial characteristics of the data.
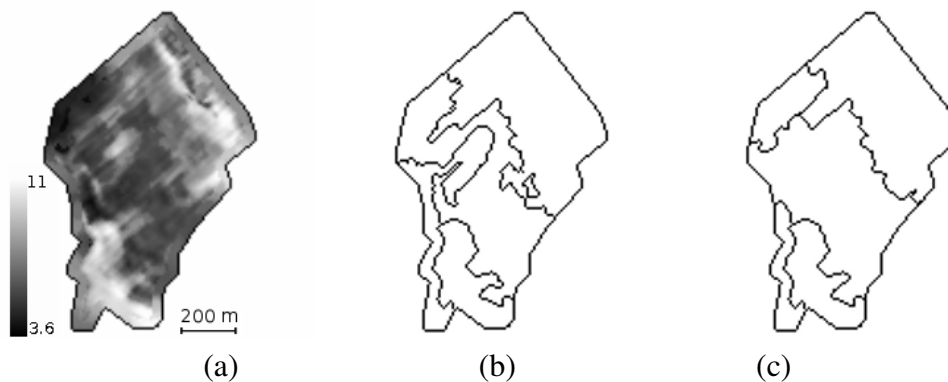

$$(a) \qquad\qquad\qquad (b) \qquad\qquad\qquad (c)$$

Fig. 9. Comparison of the efficiency of the proposed watershed segmentation using a flooding lag Δ_f: resulting SSMZ contours after regularisation. (a) Biomass values (t/ha). (b) SSMZ contours after the watershed segmentation step using the standard algorithm. (c) SSMZ contours after our watershed algorithm.

Those results show the relevance of the over-segmentation limitation method: the watershed algorithm using a flooding lag delineates wider regions. As a result: (i) the influence of the regularisation step, which is parametric, is limited in favour of the segmentation step, which is based on the data ; and (ii) it inserts a real spatial argument in the delineation of the regions, as the regularisation step processes spatial objects (*i.e.* a set of neighbouring pixels) instead of individual pixels. The over-segmentation limitation method appears to be very efficient.

Management zone delineation on the experimental fields

The approach presented was applied to the set of experimental fields. Figure 10 shows the final SSMZ results of the process after regularisation for each experimental field. From a qualitative point of view, it can be seen that main patterns of the biomass at flowering are identified for each of the four fields.
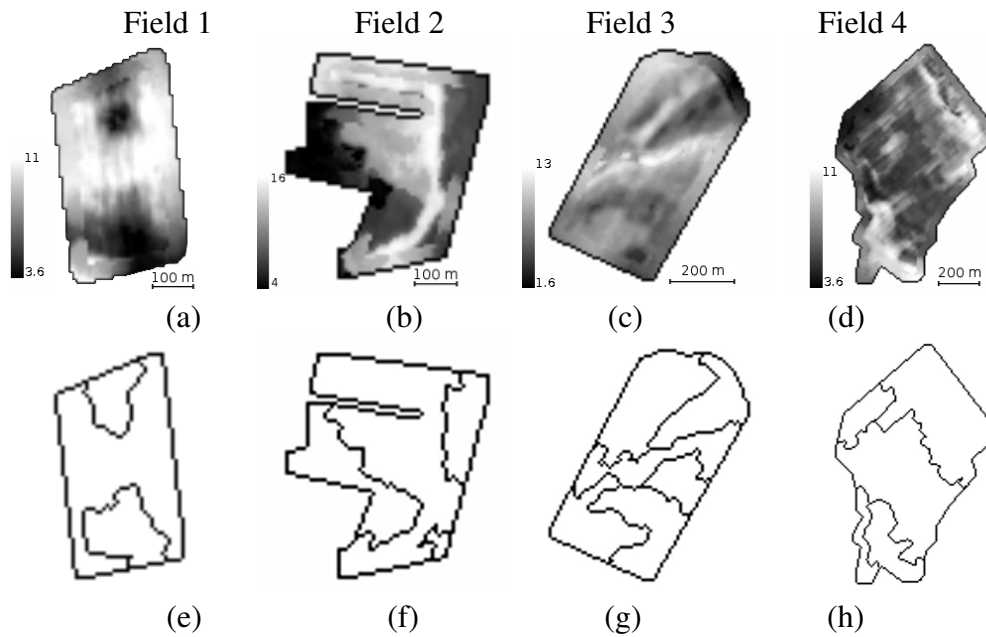
16

Field 1 Field 2 Field 3 Field 4

(a) (b) (c) (d)

(e) (f) (g) (h)

Fig. 10. Results of the SSMZ delineation using our approach. (a – d) Biomass maps (t/ha) for fields $\{1, 2, 3, 4\}$ respectively. (e – h) Resulting SSMZ for fields $\{1, 2, 3, 4\}$ respectively.

Table 1 shows that Field 2 presented the highest OI ($OI = 0.27$). Indeed, that field is characterized by a strong spatial structure and an important magnitude of the biomass variations ($S = 0.79$, $CV_a = 0.34$). As a result, SSMZ are clear because there is a reduced number of zones and an important difference in biomass values between the zones. On Field 1, the magnitude of the biomass variations is not important ($CV_a = 0.18$), but there is a very strong spatial structure of the biomass variations ($S = 0.86$). The latter facilitate the SSMZ delineation: because of this important structure of the variations, the algorithm gives satisfying contours. Three zones are obtained, *i.e.* one zone of important biomass values on the centre of the field, with two zones of weak biomass values at each end of the field. Conversely, Field 4 presents the lowest spatial structure ($S = 0.69$), and its gradient map (Figure 7.h) presents an important nugget effect. However, the magnitude of the biomass variations is important ($CV_a = 0.25$). As a result, this field presents some inclusions of high biomass value areas mixed within smaller biomass value zones, but the boundaries between zones are clear. Our algorithm succeeds in delineating SSMZ, as we found a reduced number of zones that embody such inclusions. The result is satisfactory: SSMZ gave a global view of the within-field variations. Unlike the other fields, Field 3 does not present sharp boundaries. The within-field variance is the smallest ($CV_a = 0.15$), and is not well-structured ($S = 0.69$) compared to the other fields. The gradient map (Figure 7.g) shows a reduced nugget effect. As a result, the number of delineated zones is important: our algorithm found six SSMZ. This is relevant compared to the corresponding biomass map. The boundaries of the zones are sometimes more complex than they should be: this is due to the smoothed variations of the biomass values in some parts of the field, as indicated by the low value of the OI ($OI = 0.10$). The results of our approach are also satisfactory be-

17

cause for both the watershed segmentation step and the regularisation step, computing efficiency of the algorithms allowed us to process the fields in a short time: for the experimental fields 1 to 4, segmentation time was 0.110, 0.138, 0.172, and 0.240 s respectively.

Figure 11 aims at quantifying the SSMZ delineation results for Field 1. For each management zone proposed in this field by our approach, a histogram of the biomass values is shown. The means of the biomass values within each zone are shown with a hashed line. Histograms show that populations within zones 1 and 2 on the one hand, and from zone 3 on the other hand, are significantly different from each other. While zone 3 is a wide central zone of high biomass values, biomass values of zones 1 and 2 overlap: those zones are similar in terms of their values, but are located on the two sides of the field. Finally, on field 1, we delineate 3 SSMZ corresponding to 2 different classes of biomass values.
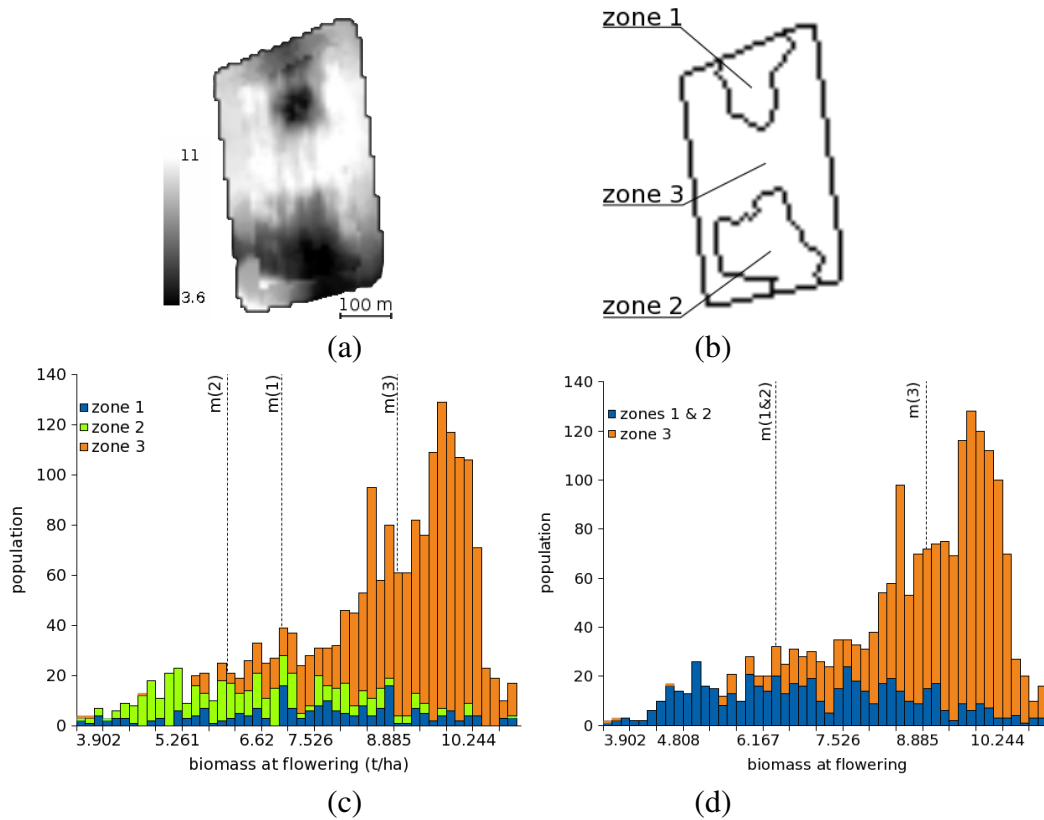

Fig. 11. Distribution of the biomass values in the management zones delineated by our approach for Field 1. (a) Biomass map (t/ha) for field 1. (b) Resulting SSMZ or field 1. (c) Distribution of the biomass values within the 3 delineated zones. (d) Distribution of the biomass values within zone 1 and 2 on one hand, zone 3 on the other hand. Mean values of the biomass data within each zone i are indicated with a hashed line and a $m(i)$ label.

18

Next steps

The object-oriented delineation approach presented in this study showed promising results. The different steps of our approach were validated. However, the tests were run on a few fields and most of the processing steps were manually supervised. Several significant problems remain. These problems currently do not allow us to implement the method as is into the production chain. One of the most significant drawbacks comes from the variogram modelling before the watershed segmentation. The variogram is a relevant way to provide an assessment of the flooding lag Δ_f. However experiments highlighted the necessity to supervise variogram estimation, which doesnt fit with the strong automation required in the context of our application. As said previously, many alternative methods can be considered (Fourier transform, wavelets, etc.) and could be tested in further experiments.

Another significant remaining problem is the determination of the optimal number of zones. The solution used in this study is relevant, but once again requires a supervision to make sure the optimal number of zones is reached. This method is lacking robustness to be fully automatable and alternative approaches will have to be investigated further. Finally, a missing functionality is the awareness of the operational constraints (*e.g.* the footprint and work direction of the application machinery).

Unlike the watershed segmentation, which gave satisfactory improvements in SSMZ delineation and which is not significantly problematic, the regularisation seems to be the most improvable step of our method. A major evolution of this step could be to include the notion of technical opportunity (Tisseyre and McBratney, 2008) into the regularisation for both (i) fusion choices during regularisation (instead of the fit parameter), and (ii) choice of the optimal number of regions (instead of using the variance decrease analysis).

Conclusion

This study showed the relevance of an object-oriented approach in SSMZ delineation. The watershed segmentation proved to be a relevant tool considering the constraints of our specific application. However, before applying this algorithm to PA data, it has to be modified in order to cope with over-segmentation effects. To be successfully implemented in production constraints like those of Farmstar (large databases, large variability in the fields to be processed), algorithms initially developed for image processing have to be specifically adapted for PA data.

19

References

Baatz, M. and Schäpe, A. (2000). Multiresolution segmentation : an optimization approach for high quality multi-scale image segmentation. In Strobl, J., Blaschke, T., and Greisebener, G., editors, *Angewandte Geographische Informationsverarbeitung XII, Beitrge zum AGIT-Symposium Salzburg*, volume 200, pages 12–23, Herbert Wichmann Verlag, Karlsruhe.

Beucher, B. and Lantuejoul, C. (1979). Use of watersheds in contour detection. In *Proceedings of the international workshop on image processing: real-time and motion detection/estimation*, Rennes, France.

Coquil, B. and Bordes, J. (2005). Farmstar: an efficient decision support tool for near real time crop management from satellite images. In Stafford, J., editor, *Proceedings of the 5th European Conference on Precision Agriculture*, pages 873–880. Wageningen Academic Publishers, Netherlands.

Doerge, T. (1999). Management zone concepts. The Site-Specific Management Guidelines. Potash and Phosphate Institute / South Dakota State University.

Fraisse, C., Sudduth, K., Kitchen, N., and Fridgen, J. (1999). Use of unsupervised clustering algorithms foir delineating within-field management zones. In *ASAE International Meeting*, Toronto, Canada. Paper 993043.

Fridgen, J., Fraisse, C., Kitchen, N., and Sudduth, K. (2000). Delineation and analysis of site-specific management zones. In Petoskey, B. J., editor, *Proceedings of the 2nd International Conference on Geospatial Information in Agriculture and Forestry*, pages 402–411, Lake Buena Vista, Florida, USA. ERIM International, Inc.

Fridgen, J., Kitchen, N., Sudduth, K., Drummond, S., Wiebold, W., and Fraisse, C. (2004). Management Zone Analyst (MZA), software for subfield management zone delineation. *Agronomy Journal*, 96:100–108.

Frogbrook, Z. L. and Oliver, M. A. (2007). Identifying management zones in agricultural fields using spatially constrained classification of soil and ancillary data. *Soil Use and Management*, 23:40–51.

Godwin, R., Wood, G., Taylor, J., Knight, S., and Welsh, J. (2003). Precision farming of cereal crops : a review of a six year experiment to develop management guidelines. *Biosystems Engineering*, 84(4):375–391.

Grimaud, M. (1992). A new measure of contrast: Dynamics. In *Proceedings of Image Algebra and Morphological Processing*, volume Proc. SPIE 1769, pages 292–305, San Diego, California, USA.

Haris, K., Efstratiadis, S. N., and Maglaveras, N. (1998). Watershed-based image segmentation with fast region merging. In *ICIP (3)*, pages 338–342.

Hornung, A., Khosla, R., Reich, R., Inman, D., and Westfall, D. G. (2006). Comparison of site-specific management zones: Soil-color-based and yield-based. *Agronomy Journal*, 98:407–415.

Jaynes, D., Colvin, T., and Kaspar, T. (2005). Identifying potential soybean management zones from multi-year yield data. *Computers and Electronics in Agriculture*, 46:309–327.

Journel, A. and Huijbregts, C. (1978). *Mining geostatistics*. Academic Press, New

York, USA.

Khosla, R., Fleming, K. L., Delgado, J. A., Shaver, T. M., and Westfall, D. G. (2002). Use of site-specific management zones to improve nitrogen management for precision agriculture. *Journal of Soil Water Conservation*, 57:513–518.

Lark, R. (1998). Forming spatially coherent regions by classification of multi-variate data: an example from the analysis of maps of crop yield. *International Journal of Geographical Information Science*, 12:83–98.

Lark, R. (2001). Some tools for parsimonious modelling and interpretation of within-field variation of soil and crop systems. *Soil and Tillage Research*, 58:99–111.

Lark, R. and Stafford, J. (1997). Classification as a first step in the interpretation of temporal and spatial variation of crop yield. *Annals of Applied Biology*, 130(1):111–121.

Li, X., Pan, Y., Zhang, C., Liu, L., and Wang, J. (2005). A new algorithm on delineation of management zone. In *Proceedings of the International Geoscience and Remote Sensing Symposium (IGARSS)*, volume 1, pages 4–8, Seoul, South Korea. IEEE International.

Li, Y., Shi, Z., Li, F., and Li, H. (2007). Delineation of site-specific management zones using fuzzy clustering analysis in a coastal saline land. *Computers and Electronics in Agriculture*, 56(2):174–186.

Matheron, G. (1963). Principles of geostatistics. *Economic Geology*, 58:1246–1266.

McBratney, A., Whelan, B., Ancev, T., and Bouma, J. (2005). Future directions of precision agriculture. *Precision Agriculture*, 6:7–23.

Meyer, F. and Beucher, S. (1990). Morphological segmentation. *Journal of Visual Communication and Image Representation*, 1(1):21–46.

Miao, Y., D.J., M., and Robert, P. (2005). Combining soil-landscape and spatial-temporal variability of yield information to delineate site-specific management zones. In Stafford, J., editor, *Precision Agriculture'05, Proceedings of the Fifth European Conference on Precision Agriculture*, pages 811–818, Uppsalla, Sweden. Wageningen Academic Publishers.

Minasny, B., McBratney, A., and Whelan, B. (2005). Vesper version 1.62. Australian Centre for Precision Agriculture, McMillan Building A05, The University of Sydney, NSW 2006.

Najman, L. and Schmitt, M. (1996). Geodesic saliency of watershed contours and hierarchical segmentation. *IEEE Transactions on Pattern Analysis and Machine Intelligence*, 18(12):1163–1173.

Patino, L. (2005). Fuzzy relations applied to minimize over segmentation in watershed algorithms. *Pattern Recognition Letters*, 26(6):819–828.

Pichel, J., Singh, D., and Rivera, F. (2006). Image segmentation based on merging of sub-optimal segmentations. *Pattern Recognition Letters*, 27(10):1105–1116.

Ping, J. and Dobermann, A. (2003). Creating spatially contiguous yield classes for site-specific management. *Agronomy Journal*, 95:1121–1131.

Plant, R. (2001). Site-specific management : the application of information technology to crop production. *Computers and Electronics in Agriculture*, 30:9–29.

Poilvé, H. and Coquil, B. (2003). Farmstar: a commercial remote sensing service to agriculture in europe. In *IGARSS'03. Proceedings of the IEEE International Geoscience and Remote Sensing Symposium*, Toulouse, France.

Pringle, M., McBratney, A., and Taylor, J. (2003). A preliminary approach to assessing the opportunity for site-specific crop management in a field, using yield sensor data. *Agricultural Systems*, 76:273–292.

Rivest, J.-F., Soille, P., and Beucher, S. (1993). Morphological gradients. *Journal of Electronic Imaging*, 2(4):326–336.

Serra, J. (1982). *Image analysis and mathematical morphology*. Academic Press, New York, USA.

Simbahan, G. and Dobermann, A. (2006). An algorithm for spatially constrained classification of categorical and continuous soil properties. *Geoderma*, 136:504–523.

Taylor, J., Wood, G., Earl, R., and Godwin, R. (2003). Soil factors ahnd their influence on within-crop variability. part ii: Spatial analysis and determination of management zones. *Biosystems Engineering*, 84(4):441–453.

Tisseyre, B. and McBratney, A. (2008). A technical opportunity index based on mathematical morphology for site-specific management: an application to viticulture. *Precision Agriculture*, 9(1-2):101–113.

Vincent, L. and Soille, P. (1991). Watersheds in digital spaces: an efficient algorithm based on immersion simulations. *IEEE Transactions on Pattern Analysis and Machine Intelligence*, 13(6):583–598.

Vrindts, E., Mouazen, A., Reyniers, M., Maertens, K., Maleki, M., Ramon, H., and de Baerdemaeker, J. (2005). Management zones based on correlation between soil compaction, yield and crop data. *Biosystems Engineering*, 92(4):419–428.

Webster, R. and Oliver, M. (1990). *Statistical methods in soil and land ressource survey*. Oxford University Press, New York, USA.

Whelan, B. and McBratney, A. (2003). Definition and interpretation of potential management zones in australia. In *Proceedings of the 11th Australian Agronomy Conference*, Geelong, Victoria. Australian Society of Agronomy.

hal-00453898, version 1 - 5 Feb 2010